ELSEVIER

Surface Science 452 (2000) 33–43

surface science

www.elsevier.nl/locate/susc

# Photoemission studies of the W(110)/Ag interface

J. Feydt, A. Elbe, H. Engelhard, G. Meister, A. Goldmann *

*Fachbereich Physik, Universität Kassel, Heinrich-Plett-Straße 40, D-34132 Kassel, Germany*

Received 5 October 1999; accepted for publication 6 January 2000

**Abstract**

We have taken normal emission photoelectron spectra using tunable synchrotron radiation from Ag overlayers grown epitaxially on W(110). One ordered monolayer (ML) exhibits four Ag-induced essentially d-like states at initial energies between 4 and 7 eV below $E_F$. Analysis of their intensity versus photon energy gives an interpretation in terms of d-like quantum well states at $E_i=(-4.2\pm0.1)$ eV, $(-4.6\pm0.1)$ eV and $(-5.0\pm0.1)$ eV and a state at $E_i=(-6.2\pm0.2)$ eV which couples strongly to a substrate bulk band. Quantum well states showing s-like character are identified at $E_i=(-3.1\pm0.1)$ eV, related to an Ag thickness of 2 ML, and at $E_i=(-2.4\pm0.1)$ eV, identified with the 3 ML film. Moreover, a d-like interface state is clearly identified at $E_i=(-1.4\pm0.1)$ eV. Besides overlayer-induced attenuation, the substrate emission appears unchanged. All photoemission features observed in our study can be uniquely identified, and this gives a solid starting point for future adsorbate studies on W(110) covered with 1 or 2 ML Ag. 

*Keywords:* Angle resolved photoemission; Low index single crystal surfaces; Metal–metal interfaces; Silver; Surface electronic phenomena (work function, surface potential, surface states, etc.); Tungsten

## 1. Introduction

For more than two decades there has been considerable interest in the electronic properties of ultrathin metal overlayers, grown epitaxially on metallic substrates [1–5]. The motivation for these studies is manifold. First it is a challenge to understand (if possible quantitatively) the transition from the one-monolayer thick adsorbate to the multilayer film representing bulk properties, i.e. the transition from the electronic 2D band structure of the ordered adlayer to the 3D bulk bands. Second, of course, the very details of the epitaxial growth process, which may change from layer to layer, are intimately connected with the electronic properties of the outermost layer(s), and any quantitative interpretation of growth modes requires information on both the surface geometry and the surface electronic properties [6,7]. Third, the interaction of very thin metallic adlayers with gaseous adsorbates may be very different compared with the clean (bulk) single crystal surfaces of the substrate and also of the adsorbate material [8]; this gives some hope that reaction properties may be tailored by adequate combinations of different materials. In addition the question arises of whether particular electronic interface states are created and located spatially just at the boundary between substrate and adsorbate film. Finally, under special conditions, quantum well states may be observed which result from standing electron waves trapped [9–11] between the surface barrier

* Corresponding author. Fax: +49-561-804-4518.
*E-mail address:* goldmann@physik.uni-kassel.de (A. Goldmann)

0039-6028/00/$ - see front matter 
PII: S0039-6028(00)00294-6

on the vacuum side and a bandgap on the substrate side, see e.g. Refs. [5,7,12–14].

W(110) is an experimentally convenient substrate for the epitaxial growth of several metals and metal alloys. In particular with noble metal overlayers no alloying occurs and the sample can be cleaned after each deposition step just by thermal desorption of the adsorbate. We have started a systematic study of ultrathin noble metal overlayers on W(110) and their interaction with gaseous adsorbates. With this aim we have first analyzed the clean W(110) surface and the bulk band structure along the surface normal, employing normal emission photoelectron spectroscopy [15]. The vibrational modes of oxygen chemisorbed dissociatively on W(110) were studied by high-resolution electron energy-loss spectroscopy [16]. Atomic oxygen induces drastic changes of the photoemission spectra in the energy region of the substrate valence bands, and these have been investigated recently employing tunable synchrotron radiation [17]. In an earlier study we observed an adsorbate-driven rearrangement of a metal overlayer: exposure of one closed monolayer of Ag on W(110) to molecular oxygen at room temperatures results in clean Ag islands two layers thick and open W(110) areas covered with an ordered atomic oxygen overlayer [18]. In this work [18] we exploited the fact that photoemission spectra can safely distinguish between a one-monolayer and a double-layer of Ag on W(110), and this gave the opportunity to use the shape of the electron distribution curves just as a fingerprint. The present study tries to understand monolayer Ag films on W(110) with respect to their electronic properties.

## 2. Experimental

The W(110) crystal was oriented to $\pm 0.25^\circ$. It was 1.5 mm thick and had a diameter of about 10 mm. This sample was mounted between two tungsten rods and may be heated from the rear by electron bombardment. Cleaning proceeds by heating in an oxygen atmosphere ($5 \times 10^{-8}$ Torr) at a temperature of 1400 K and a subsequent flash to 2300 K. Cleanliness was controlled by the absence of contamination lines in core-level photoelectron spectra (excited with Al K$\alpha$ radiation at $\hbar\omega = 1487$ eV), sharp low energy electron diffraction (LEED) spots with low background intensity and the absence of spots due to carbon overlayers, and (perhaps most sensitive) the presence of a sharp surface resonance at an initial state energy $E_i = -1.2$ eV in the valence band photoemission spectra [15,19]. Contamination from the residual gas pressure in the experimental chamber ($8 \times 10^{-11}$ Torr) could be removed by a short flash to 2300 K.

Normal emission photoelectron spectra were excited using the 3 m normal incidence monochromator (NIM 1) beamline at the storage ring BESSY in Berlin. The correct orientation of the sample normal was checked optically by reflection of a visible He–Ne laser beam through the electron energy analyzer and several windows of the vacuum chamber. The input lens of the hemispherical energy analyzer is equipped with an input aperture which allows in situ variation of the angular resolution between $\Delta\theta = \pm 1^\circ$ and $\pm 12^\circ$. In general data were taken at $\Delta\theta = \pm 2^\circ$. If not specified differently the electron spectra were recorded at a total energy resolution $\Delta E = 80$–100 meV including the contribution from the monochromator. Light is about 90% p-polarized and impinges onto the sample at $60^\circ$ with respect to the sample normal and with the electric field component parallel to the surface oriented along the [001] direction of the bulk lattice. The experiments with He resonance radiation ($\hbar\omega = 21.2$, 40.8 eV) and Al K$\alpha$ radiation were performed in an apparatus located in our home laboratory — this is described in detail elsewhere [18]. In that case the resolution parameters were set to $\Delta\theta = \pm 2^\circ$ and $\Delta E = 50$ meV, respectively. With both spectrometers spectra were always taken at room temperature.

Ag was evaporated from an alumina crucible, always at a constant rate of 0.2 ML/min, with the substrate at room temperature. The evaporation rate was controlled by a quartz microbalance. Relative Ag coverages were measured by the X-ray photoelectron spectroscopy (XPS) intensities of the Ag 3d and W 4d core levels. The absolute calibration relies on a combination of LEED and ultraviolet photoelectron spectroscopy (UPS)

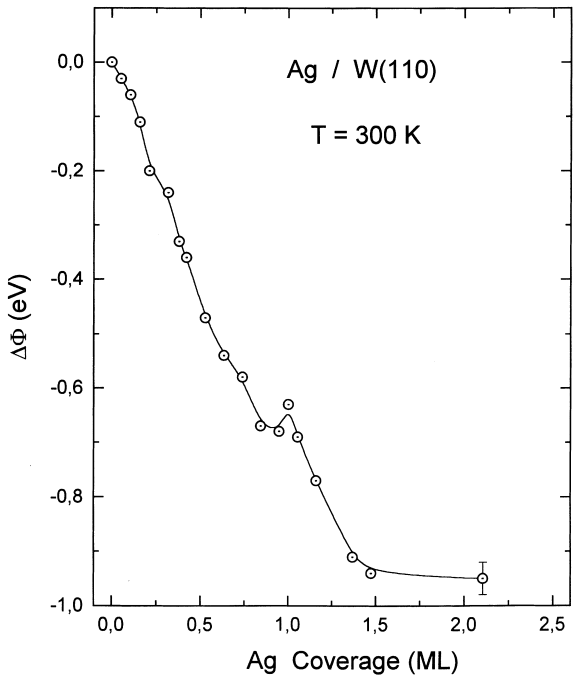


Fig. 1. Change of the work function with Ag coverage. Relative error in $\Delta\Phi$ is independent of coverage and is indicated at about 2.1 ML coverage.

results as well as on the Ag-induced change in work function $\Delta\Phi$. We estimate the calibration of coverage to be accurate to about 15% of a monolayer. The work function was determined from the shift of the low energy cut-off of the electron energy distribution curve, with a negative voltage of 9 V applied to the sample. Our $\Delta\Phi$ results are reproduced in Fig. 1. A kink appears just at 1 ML, in agreement with earlier results of other authors [20,21]. Our $\Delta\Phi$ values are generally larger by 50 to 100 meV compared with Refs. [20,21]. We attribute this to improved vacuum conditions in our work.

## 3. Results and discussion

The growth modes of Ag on W(110) have already been studied earlier [20,22–25]. The atomic radius of Ag exceeds that of W considerably. Therefore Ag does not grow pseudomorphically, but forms an incommensurate first monolayer. This is made evident by the complex LEED pattern which we observe in agreement with Ref. [20]. LEED and Auger spectroscopy studies demonstrate the growth of a second layer on top of the closed first one [20,23]. Thermal desorption spectra show that the first two layers are stable up to their desorption temperature, but with the second layer bound less strongly than the first one [20]. The buckling amplitude of the first two layers was studied using helium atom diffraction [25]. It was found to be smaller than expected from a hard-sphere model. The structural analysis [25] indicates an expansion (contraction in the other direction) of the real-space surface unit cell of 10% (3%) at most. Thus both the monolayer and the bilayer can be viewed to first order as an approximate fcc(111) surface, very similar to Ag(111), but distorted in order to better match the substrate geometry. Further Ag deposition ($\geq 3$ ML) leads to growth of three-dimensional crystallites on top of the essentially closed bilayer, with the (111) plane oriented parallel to the substrate surface. Since (at all coverages) domains with different (but crystallographically equivalent) orientations were observed [20], we have only studied normal emission photoelectron spectra to avoid any ambiguity. Where comparable our data generally agree with earlier observations. However, our results are taken at both good energy and angular resolution. Therefore they allow a rather detailed interpretation as shown below.

Coverage-dependent submonolayer spectra excited at two photon energies are reproduced in Fig. 2. The clean substrate exhibits W(5d) emission at initial state energies $E_i$ between $E_F$ and $-3$ eV. No structural features are resolved at $-8\text{ eV} < E_i < -3\text{ eV}$. This is shown in Fig. 2a for $\hbar\omega = 40.8$ eV and was also observed (not reproduced) at $\hbar\omega = 21.2$ eV. With increasing coverage the substrate 5d-band emission at initial state energies $E_i$ between $E_F$ and $-4$ eV is suppressed as expected. Ag-induced emission lines are observed between $E_i = -4$ and $-7$ eV. Their intensities increase linearly with Ag coverage as expected. To make the low coverage lines better visible, all spectra in Fig. 2 have been normalized to equal maximum amplitudes. Using two different photon energies we can clearly resolve four

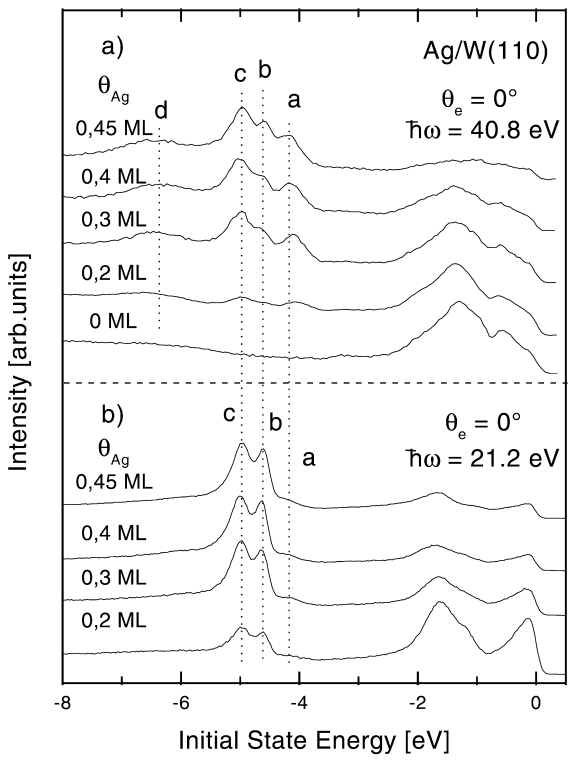


Fig. 2. Electron energy distribution curves taken in normal emission from W(110) covered with different submonolayer quantities of Ag: (a) photon energy $\hbar\omega = 40.8$ eV, (b) $\hbar\omega = 21.2$ eV. All spectra taken at room temperature and plotted normalized to equal maximum amplitude.

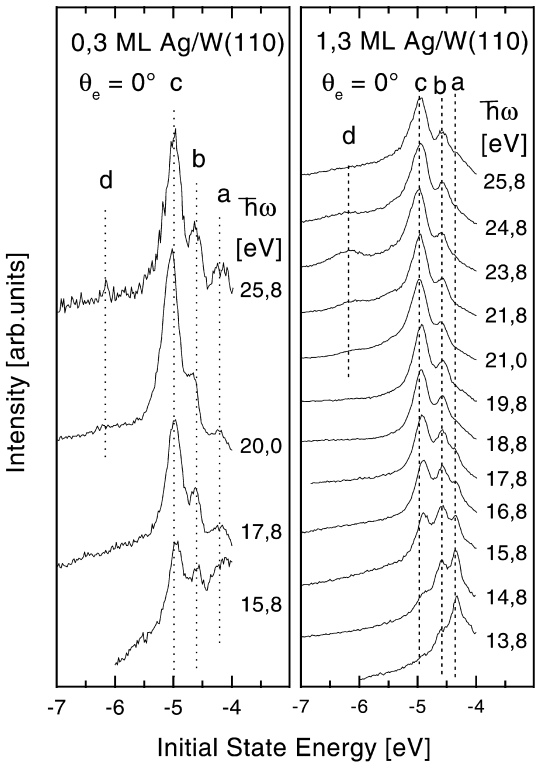


Fig. 3. Normal emission spectra taken at different photon energies $\hbar\omega$ from 0.3 ML Ag on W(110), left panel, and 1.3 ML Ag on W(110), right panel. The intensities are plotted to make relevant features visible and do not reproduce the $\hbar\omega$-dependent count rates as measured.

different emission peaks a, b, c and d which, however, differ considerably with respect to intensities and linewidths. At fixed $\hbar\omega$ they do not change their relative shapes, and we interpret this as a clear fingerprint of the growth of monolayer islands with increasing diameter. This is in agreement with earlier structural studies [20,23], which show a very different Ag intensity distribution between $-4$ and $-6$ eV at 2 ML coverage. Decomposition of the Ag emission features indicates (not shown) that peaks a, b and c have an experimental linewidth between 0.2 eV (b) and 0.3 eV (a, c), while peak d is more than 1 eV broad. Also the relative intensities of peaks a and d compared with b and c depend sensitively on $\hbar\omega$, and this indicates a different orbital composition of the electron states involved.

We have therefore studied the $\hbar\omega$ dependence in more detail. In the following we concentrate on the $E_i$ range between $-4$ and $-8$ eV. Fig. 3 (left panel) reproduces some spectra taken at fixed coverage but varying photon energy. In agreement with Fig. 2 three structures are resolved at $E_i = -(4.2 \pm 0.1)$ eV (peak a), $E_i = -(4.6 \pm 0.1)$ eV (peak b) and $E_i = -(5.0 \pm 0.1)$ eV (peak c). In contrast, peak d is not clearly identified. The latter structure shows a narrow resonance-like intensity enhancement around $\hbar\omega = (23.8 \pm 0.5)$ eV, see the results reproduced in the right panel of Fig. 3. These spectra were taken at somewhat worse energy resolution compared with the left panel, and also at Ag coverage somewhat exceeding 1 ML; nevertheless the structures a–d are still dominated by those characteristic of the submonolayer spectra. This is consistent with the structural information [20,23] that the second Ag layer grows

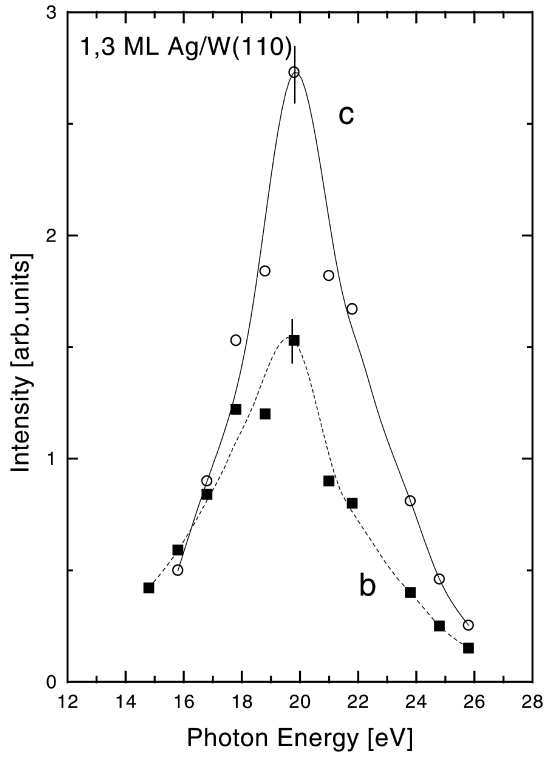


Fig. 4. Relative variation of peak amplitudes with photon energy $\hbar\omega$. Top curve corresponds to peak c, bottom curve to peak b in Fig. 3.

epitaxially on top of the first one. The intensity resonance of peak d indicates the possible existence of a resonant initial state at $-6.2$ eV or a resonant final state at $E_f = E_i + \hbar\omega = (17.6 \pm 0.7)$ eV.

The spectra reproduced in Fig. 3 are plotted with different intensity scales to make the peak positions a–d better visible. In order to evaluate intensity variations with $\hbar\omega$, however, all spectra were normalized to the incoming photon flux, a linear background subtraction was performed and, since the linewidths did not depend on $\hbar\omega$, the remaining peak maximum amplitude was taken as a measure of peak intensity. The results of this analysis are summarized in Fig. 4. Peak b is resonant at $\hbar\omega = (19.4 \pm 0.5)$ eV, corresponding to a final state energy $E_f = (14.8 \pm 0.5)$ eV. Similarly we observe a resonance maximum at $\hbar\omega = (19.9 \pm 0.5)$ eV for peak c, with a resulting energy $E_f = (15.0 \pm 0.5)$ eV. Before we try an interpretation of the observed $I(\hbar\omega)$ resonances let us first inspect the electronic structure of the tungsten substrate. Normal emission from two-dimensional electronic states corresponds to the center of the surface Brillouin zone. Normal emission from 3D bulk bands corresponds to photoelectron emission from $E(k)$ points located on the Γ–N line of the bcc Brillouin zone. The relevant bands are reproduced in Fig. 5. Several aspects are of relevance.

First there is an energy gap between $E_i = -3.4$ and $-6.2$ eV. This means that the initial states labeled a, b, c in Figs. 2 and 3 cannot couple

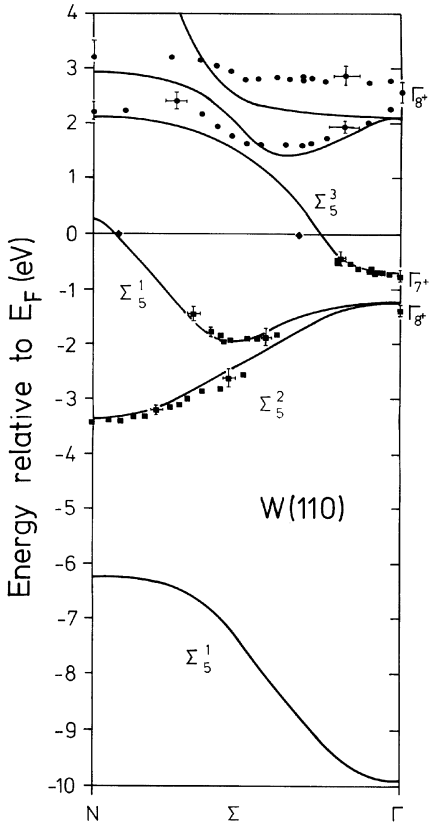


Fig. 5. Section of the electronic energy band structure of tungsten along the Γ–Σ–N symmetry direction of the bulk Brillouin zone. The solid lines reproduce calculations by Christensen and coworkers [26,27] using a relativistic augmented plane-wave method. Data points are from angle-resolved inverse photoemission [28] and photoemission [15], respectively. The upper symmetry labels refer to single-point group symmetry neglecting spin–orbit coupling, the lower indices refer to the relativistic double-group classification including spin–orbit interactions.

directly to the substrate, i.e. they do not extend deep into tungsten but are spatially confined to the Ag overlayer. Therefore these 'isolated' 4d-orbitals can interact only laterally with neighbouring Ag atoms and may be characterized as d-like quantum well states. This explains the observed small linewidths.

Second the peak labeled d ($E_i = -6.2$ eV) in Figs. 2 and 3 clearly overlaps energetically with a tungsten bulk state in the vicinity of N. In fact also the Ag bulk band structure shows a nearly dispersionless (i.e. essentially atomic-like) d-band around $E_i = -6$ eV [29,30]. Due to its localized character we may expect its existence at comparable $E_i$ also within the silver monolayer. This orbital obviously hybridizes with $\Sigma_5^1$ substrate states around N. These are of s, $d_{z^2}$-like orbital character. Due to this coupling a d-like photohole localized within the Ag layer is filled rapidly from below. Consequently its lifetime is reduced considerably and this is observed in the increased (inverse lifetime) width (at least a factor of five compared with the quantum well d-states). Our interpretation is furthermore supported strongly by the observed intensity resonance of peak d pointing to a final state at $E_f = (17.6 \pm 0.7)$ eV. Christensen and coworkers' band structure calculation [26,27], which was experimentally proven to be correct above $E_F$ within at least typically 1 eV [15], predicts a bulk final state band with $E_f = 17.2$ eV just at N. This may be excited resonantly from the occupied $\Sigma_5^1$ bulk band around N with photons of $\hbar\omega = 23.4$ eV. Due to the hybridization with these bulk states the photoemission peak d is coupled to the corresponding intensity resonance, which was observed experimentally at $\hbar\omega = (23.8 \pm 0.5)$ eV.

In contrast to peak d, emission lines b and c are resonant both with a final state around $E_f = 15$ eV, different from d. Although it is tempting to identify this with a critical Γ-point of bulk tungsten observed at $E_f = (15.3 \pm 0.5)$ eV [15], we do not believe this to be correct. Since b and c are localized energetically within a wide gap of the projected bulk band structure, they should not couple to bulk states. Instead we conjecture an atomic-like d→f transition within the Ag monolayer to an f-orbital around $E_f = 15$ eV. Such an orbital can be identified around 15–17 eV in the calculated band structure of bulk Ag [29] and it should exist at similar energies also for atomic Ag and a 2D Ag overlayer.

There are several other studies of ultrathin Ag layers on transition metal substrates [1,3,4,14, 31,32]. Most of them are concentrated on narrow emission features around 4–6 eV below $E_F$. Some corresponding photoelectron data obtained from ordered overlayers in normal emission geometry are collected in Table 1. As is evident, both absolute energy positions and energy differences between Ag-induced peaks appear very similar. This is not accidental. In almost all cases Ag grows in the form of a somewhat laterally distorted hexagonal overlayer. Therefore, since the Ag—Ag

Table 1
Ag-induced photoemission peaks (a–d) observed from an Ag monolayer deposited on various substrates. Error bars typically ±1–2 in units of last digit unless otherwise indicated

| Substrate | $-E_i$ (eV) | | | | Reference |
|---|---|---|---|---|---|
| | a | b | c | d | |
| W(110) | 4.2 | 4.6 | 5.0 | 6.2(2) | this work |
| Cu(100) | 4.2 | 4.7 | 4.9 | 6.5 | [31,32] |
| Ni(111) | | 4.6 | 5.9 | 6.4 | [3] |
| V(100) | | 4.4(3) | 5.0(2) | 6.3(2) | [14][a] |
| Pt(111) | | 4.5 | | | [4] |
| Cu(111) | | | 4.9 | 6.6 | [3] |
| Au(111) | 3.8 | | 4.9 | 6.1 | [3] |
| Ni(100) | | ~4.6 | | | [3] |

[a] Extracted by us from fig. 1 of Ref. [14].

distances are not too different, the lateral overlap is similar and the resulting crystal-field splitting will be comparable too. Of course the spin–orbit interaction energies, typically 0.2 eV in Ag, will also mix in. Tobin et al. [32] made a qualitative symmetry analysis by simply assuming a perfect hexagonal ($C_{6v}$) arrangement. They propose a d-orbital assignment of $(3z^2-r^2)$ to peak a and ($xz$, $yz$) to b and c. Finally they attribute s-like character to d. This interpretation is fully consistent with our results presented above: if peak d carries s ($+z^2$) character, its coupling to substrate orbitals at N is allowed by symmetry. Also peaks a, b and c should be separated energetically under the action of the 2D crystal-field within the $C_{2v}$ Ag overlayer.

We note in passing that we also studied Ag films at a nominal thickness of 3, 5, 10 and 30 ML. Already at 3 ML a band is resolved around $E_i=-5$ eV which shows some dispersion with $\hbar\omega$, i.e. some 3D character. This is more pronounced at 5 ML. In both cases, intensity maxima $I(\hbar\omega)$ were resolved which differ in their peak position from both the 1 ML results and the results obtained for clean W(110). At 10 and 30 ML we observed all features characteristic for (111) surfaces of bulk Ag crystals: they exhibit the 'correct' dispersion $E_i$ ($\hbar\omega$) in normal emission [30], they show the intensity resonances $I(\hbar\omega)$ well known for Ag(111) [30], and our home laboratory experiments (performed at excellent angular resolution) also clearly resolve the Shockley-type surface state at $E_i=-0.05$ eV. From this we conclude that thicker layers of Ag on W(110), although they grow as three-dimensional crystallites on top of the closed bilayer, form sufficiently large (111) terraces to allow the existence of the surface state.

In the following we concentrate on Ag-induced photoemission peaks within the substrate valence band region. No prominent new features can be observed at coverages up to about 1 ML, compare Fig. 2. At increasing film thickness, a new peak labeled H appears at $E_i=-3.1$ eV, see Fig. 6. It is obviously related to the double-layer. Generally three interpretations seem possible: peak H may result from a quantum well state (s-like electron waves within the Ag film, with wave-vector parallel to the surface normal), or it results from an

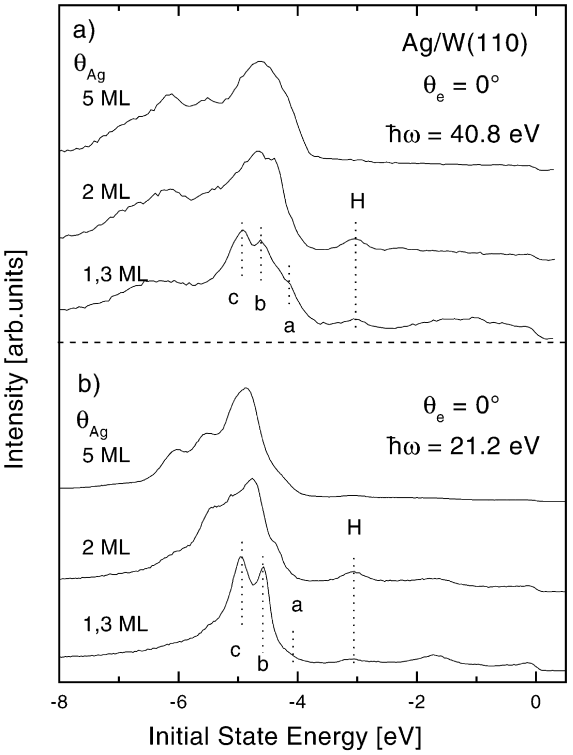


Fig. 6. Electron energy distribution curves taken in normal emission from W(110) covered with Ag layers of different thickness: (a) $\hbar\omega=40.8$ eV, (b) $\hbar\omega=21.2$ eV. All data taken at room temperature and plotted normalized to equal maximum amplitude.

interface state (an Ag orbital couples strongly to a substrate level causing a spatially localized state), or H results from a Shockley-type surface state (residing on the vacuum side of the overlayer and penetrating exponentially damped into an energy gap within the substrate bulk bands).

To obtain more information we have studied the intensity of peak H in its dependence on $\hbar\omega$. Typical spectra are shown in Fig. 7. Here we reproduce data normalized to equal amplitude. This type of plot enhances weak peaks and makes the identification of dispersion effects with $\hbar\omega$ easier. Of course the plot of Fig. 7 does not allow a realistic estimate of intensities. To obtain these, all data were also normalized to the incoming photon flux, and peak amplitudes (after subtraction of a linear background) were taken as a measure of intensities. The intensity variation $I(\omega)$

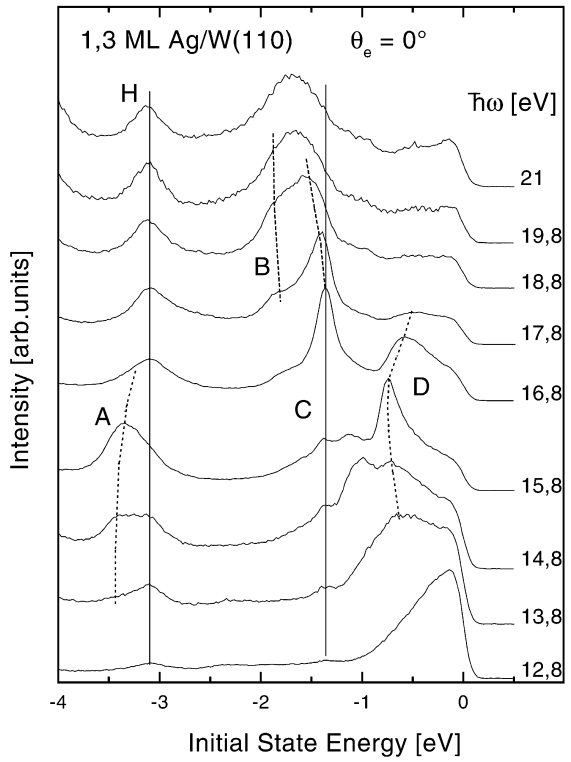


Fig. 7. Normal emission spectra taken at different photon energies from 1.8 ML Ag on W(110). $T=300$ K, spectra plotted normalized to equal maximum amplitudes.

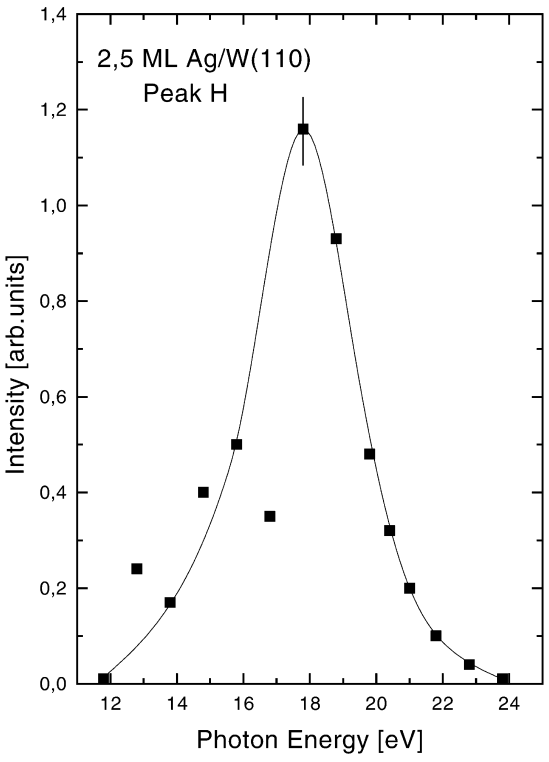


Fig. 8. Relative variation of the amplitude of peak H with photon energy indicating a resonance-like intensity maximum at $\hbar\omega=(18\pm1)$ eV.

of peak H is shown in Fig. 8, indicating a resonance at $\hbar\omega=(18\pm1)$ eV. The position of this maximum most probably rules out an interpretation in terms of an interface state. Inspection of Fig. 5 suggests that an interface state would couple to the bulk states at the N-point ($E_i=-3.4$ eV). In consequence we should expect a resonance essentially at the energy of the corresponding bulk to bulk band transition at N observed for clean W(110) [15]. This, however, was identified experimentally at $\hbar\omega=(15.7\pm0.5)$ eV. Therefore we rule out an interface state.

A Shockley-type surface state could in principle exist at the Ag overlayer. Its symmetry should be $\Sigma_5^1$ and inspection of Fig. 5 clearly indicates that a gap of states with the corresponding symmetry exists between $E_i=-2$ and $-6.2$ eV along $\Gamma$N. However, a careful investigation of surface states residing on ultrathin silver islands on graphite [12] shows that their binding energies never exceed 1 eV. This observation makes a surface state at $E_i=-3.1$ eV highly improbable. Therefore only an interpretation of peak H as a quantum well state confined to the Ag double-layer is possible. The corresponding electrons are trapped between the surface barrier at the vacuum side and the $\Sigma^1$-like symmetry gap on the substrate side. We also identified a second quantum well state observed at $E_i=-2.4$ eV and connected with the 3 ML Ag overlayer (not shown). Its intensity is very large at $\hbar\omega=12.8$ eV, goes through a minimum and shows a resonance around $\hbar\omega=(17.2\pm1)$ eV, indicating a relevant final state at $E_f=(14.8\pm1)$ eV.

While our interpretation of quantum well states (QWS) so far is based exclusively on experimental

arguments, strong additional support results from solving the phase accumulation model [33,34]. This model has been applied [34] to the case of QW states in epitaxial layers of Ag on Fe(100): the quantization condition for the existence of standing waves in the QW is

$$\Phi_C(E) + 2k(E)d + \Phi_B(E) = 2\pi n$$

where $\Phi_C$ and $\Phi_B$ are the phase changes on reflection at the crystal (C) hybridization gap and at the surface barrier (B) produced by the electron image potential, and where $k$ is the wave-vector of a free electron propagating in an Ag layer of thickness $d$. The total phase accumulation must be an integer multiple of $2\pi$ [34]. To apply this conceptually transparent model to our experiment we have used the formulas (5) and (6) given in Ref. [34] to calculate $\Phi_B$ and $\Phi_C$. In our case we used the parameters $E_V = 5.2$ eV [position of vacuum level of W(110)] and the appropriate $\Delta\Phi$ values taken from Fig. 1 to model the work function of the overlayer. Similarly $\Phi_C$ was evaluated with the parameters taken from Fig. 5 of our paper: $E_L = -6.2$ eV and $E_U = -1.9$ eV characterize the lower (L) and upper (U) edges of the substrate $\Sigma_5^1$ hybridization gap. To generate $2kd$ we have calculated $k$ from the standard two-band nearly-free electron expression, based on eq. (7) of Ref. [34]. Of course we have modified this equation to apply along the (111) direction of Ag, assuming a (111)-fcc growth of Ag on W(110), and adjusting the parameters to reproduce the known band energies along the (111) direction of Ag: $L_{4'} = -0.6$ eV and $L_1 = +3.8$ eV.

The phase accumulation model predicts the QW states surprisingly accurately. At 1 ML coverage the calculation gives an eigenvalue at $-3.9$ eV. At 2 ML we calculate $E_i = -2.8$ eV, to be compared with the experimental result $E_i = -3.1$ eV. Similar good agreement is found for 3 ML: the model predicts $E_i = -2.2$ eV, to be compared with the experimental peak at $-2.4$ eV. The result obtained for 1 ML indicates that peak a, observed at $E_i = -4.2$ eV, may not be purely d-like. The interpretation presented before [32] identifies peak a with a d-like state showing $(3z^2 - r^2)$ orbital character. This symmetry allows admixtures of s-like electron density, consistent with the orbital character of a QW state. Without more specific calculations we are not able to interpret peak a in more detail. Our simple model calculation predicts additional QW states at $E_i = -4.7$ eV (2 ML) and $-3.9$ eV (3 ML). These, however, are not resolved in our data. They are masked by intense (d-like) emission and/or are excited only weakly in our photon energy range.

Quantum well states and their intensity variations with photon energy $\hbar\omega$ have already been reported and discussed in several papers [35–38]. The intensity oscillations with $\hbar\omega$ are ascribed to the interference between the contributions to the outgoing wave associated with the two tails of a QW state [36]. In this model the main effect is coherent interference of the surface and interface photoemission [37]. It is not at all trivial to make this model quantitative for our experiments. In fact the intensity resonance observed in Fig. 8 was only exploited by us to indicate that no coupling to a resonating bulk state can explain peak H. Unfortunately our data points in Fig. 8 are not sufficiently dense on the energy scale to rule out (or not) additional weaker resonances around $\hbar\omega = 15.7$ and 12.8 eV. Such rapid oscillations could be consistent with the interference model [37].

The structures labeled A, B, D in Fig. 7 and connected by dashed lines are due to substrate bulk emission and have been interpreted elsewhere [15]. Peak C is a clearly identified interface state. It is observed at $E_i = -1.4$ eV in Fig. 7. On clean W(110), a corresponding surface resonance (SR) is identified at $E_i = -1.2$ eV [15,19], with an intensity resonance at $\hbar\omega = 16$ eV. Fig. 7 (and a more detailed analysis based on normalization to the incident photon flux) shows that peak C resonates at the same photon energy, indicating a common origin. The origin of SR on clean W(110) was interpreted as follows: due to the potential at the outermost layer, which is different from the bulk, SR is split off a bulk band. In consequence it carries dominant d-orbital character and is located spatially at the surface layer. Obviously adsorption of Ag induces some charge transfer from Ag to W, this modifies the surface potential additionally and shifts the former SR to the position of C. This explains C as an interface state. Our interpretation

is supported by two observations. First, C is observed in spectra taken from 1, 2 and 3 ML Ag films (but with varying relative intensity). Second, chemisorption of atomic oxygen on clean W(110), which induces charge transfer from W to oxygen, shifts SR by about 0.2 eV but in the opposite direction [17].

## 4. Conclusions

Our results may be summarized as follows. The epitaxial growth of Ag on W(110) at room temperature proceeds in complete agreement with earlier results of other groups. From normal emission photoelectron spectra taken with tunable synchrotron radiation we report the following new results. One ordered monolayer of Ag on W(110) exhibits four Ag-induced essentially d-like states at initial state energies between 4 and 7 eV below $E_F$. The most tightly bound of these (s, $d_{z^2}$-like) has an experimental linewidth $>1$ eV and is shown to hybridize strongly with an energetically underlying substrate orbital. The other three are located energetically within an energy gap of the surface-projected bulk band structure. They therefore do not couple normal to the surface but show an essentially atomic behaviour (line widths 0.2 to 0.3 eV). Their energetic positions seem to be governed by the combined action of lateral crystal-field splitting and spin–orbit interaction. Within the energy region of intense substrate valence band emission (0–4 eV below $E_F$) we have clearly identified a d-like interface state at 1.4 eV below the Fermi energy, which is connected with the first monolayer. At 2 ML coverage, an s-like quantum well state can be identified at an initial state energy $E_i = -3.1$ eV. A second quantum well state appears at $E_i = -2.4$ eV in 3 ML of Ag. Besides overlayer-induced attenuation, the substrate emission appears unmodified. This is a clear indication that no relevant reconstruction is induced by the Ag deposit. In conclusion, all features observed in normal emission photoelectron spectra at various photon energies can be interpreted. This gives a solid basis for the study of adsorbate interactions with Ag monolayers on W(110).

## Acknowledgements

This work was supported by the Bundesministerium für Bildung und Forschung (BMBF). We thank Ch. Jung and W. Braun and the BESSY staff for help. A.E. acknowledges a generous grant from the 'Otto-Braun-Stiftung'. The experiments in our home laboratory are continuously supported by the Deutsche Forschungsgemeinschaft (DFG).

## References

[1] K. Jacobi, in: S.D. Kevan (Ed.), Angle-Resolved Photoemission, Theory and Current Applications, Elsevier, Amsterdam, 1992, p. 371. Chapter 10.
[2] S.D. Kevan (Ed.), Angle-Resolved Photoemission, Theory and Current Applications, Elsevier, Amsterdam, 1992.
[3] A.P. Shapiro, T.C. Hsieh, A.L. Wachs, T. Miller, T.-C. Chiang, Phys. Rev. B 38 (1988) 7394.
[4] B. Schmiedeskamp, B. Kessler, B. Vogt, U. Heinzmann, Surf. Sci. 223 (1989) 465.
[5] T. Valla, P. Pervan, M. Milun, F.B. Hayden, D.P. Woodruff, Phys. Rev. B 54 (1996) 11 786.
[6] H. Brune, Surf. Sci. Rep. 31 (1998) 121.
[7] N. Memmel, Surf. Sci. Rep. 32 (1998) 91.
[8] J.A. Rodriguez, Surf. Sci. Rep. 24 (1996) 223.
[9] N.V. Smith, D.P. Woodruff, Progr. Surf. Sci. 21 (1986) 295.
[10] N.V. Smith, Rep. Progr. Phys. 51 (1988) 1227.
[11] P.M. Echenique, J.B. Pendry, Progr. Surf. Sci. 32 (1990) 111.
[12] F. Patthey, W.-D. Schneider, Surf. Sci. 334 (1995) L715.
[13] J.J. Paggel, T. Miller, T.-C. Chiang, Phys. Rev. Lett. 81 (1998) 5632.
[14] P. Pervan, M. Milun, D.P. Woodruff, Phys. Rev. Lett. 81 (1998) 4995.
[15] J. Feydt, A. Elbe, H. Engelhard, G. Meister, A. Goldmann, Phys. Rev. B 58 (1998) 14 007.
[16] A. Elbe, G. Meister, A. Goldmann, Surf. Sci. 371 (1997) 438.
[17] J. Feydt, A. Elbe, H. Engelhard, G. Meister, A. Goldmann, Surf. Sci. 440 (1999) 213.
[18] A. Elbe, G. Meister, A. Goldmann, Surf. Sci. 397 (1998) 346.
[19] R.H. Gaylord, S.D. Kevan, Phys. Rev. B 36 (1987) 9337.
[20] E. Bauer, H. Poppa, B. Todd, P.R. Davis, J. Appl. Phys. 48 (1977) 3773.
[21] Y.B. Zhao, R. Gomer, Surf. Sci. 280 (1993) 138.
[22] E. Bauer, Appl. Surf. Sci. 11/12 (1982) 479.
[23] E. Bauer, H. Poppa, Thin Solid Films 121 (1984) 159.

[24] H. Gollisch, Surf. Sci. 175 (1985) 249.
[25] Y. Yang, H. Xu, T. Engel, Surf. Sci. 276 (1992) 341.
[26] N.E. Christensen, B. Feuerbacher, Phys. Rev. B 10 (1974) 2349.
[27] R.F. Willis, N.E. Christensen, Phys. Rev. B 18 (1978) 5140.
[28] D. Li, P.A. Dowben, J.E. Ortega, F.J. Himpsel, Phys. Rev. B 47 (1993) 12 895.
[29] H. Eckardt, L. Fritsche, J. Noffke, J. Phys. F.: Met. Phys. 14 (1984) 97.
[30] H. Wern, R. Courths, G. Leschik, S. Hüfner, Z. Phys. B 60 (1985) 293.
[31] J.G. Tobin, S.W. Robey, L.E. Klebanoff, D.A. Shirley, Phys. Rev. B 28 (1983) 6169.
[32] J.G. Tobin, S.W. Robey, D.A. Shirley, Phys. Rev. B 33 (1986) 2270.
[33] N.V. Smith, Phys. Rev. B 32 (1985) 3549.
[34] N.V. Smith, N.B. Brookes, Y. Chang, P.D. Johnson, Phys. Rev. B 49 (1994) 332.
[35] A. Carlsson, D. Claesson, G. Katrich, S.-A. Lindgren, L. Walldén, Surf. Sci. 352–354 (1996) 656.
[36] A. Carlsson, D. Claesson, D.-A. Lindgren, L. Walldén, Phys. Rev. B 52 (1995) 11 144.
[37] M. Milun, P. Pervan, B. Grumhalter, D.P. Woodruff, Phys. Rev. B 56 (1999) 5170.
[38] J.J. Paggel, T. Miller, T.-C. Chiang, J. Electron Spectrosc. Relat. Phenom. 101–103 (1999) 271.